Cellular cargo manipulation using magnetically steerable microrobots in dense environments

Abstract

This study presents a microrobotic system that utilizes magnetic Janus microrobots and a 3D-printed magnetic tweezer setup controlled by electromagnetic coils to transport cells in a densely crowded environment. The system was successfully demonstrated to transport cells in a densely populated sample of cells. The results indicate that this microrobotic system could address challenges such as off-target delivery, thereby realizing the full potential of medical microrobots for this and other applications. This study represents an important step towards developing a more efficient and effective method for targeted drug delivery in the field of medicine.

Introduction

Microrobots actuated by non-toxic sources are gaining widespread interest in biomedicine.[1] Despite the recent groundbreaking discoveries in biomedicine, challenges such as high dosage with complicated side effects and off-target distribution greatly hinder the promised benefits. Therefore, the targeted delivery of therapeutics, such as cells, drugs, genetic material, etc., is highly desired for the next generation of disease prevention and cure.[2] In recent years, magnetically controlled microrobots have been investigated as promising candidates for delivering cargo in biological environments.[3] Substantial progress has been made in the fabrication,[4] propulsion,[5] and imaging[6] of these microbots for medicine. However, biomedical robotic applications have been limited to targets with relatively easy access, such as inside the eyes[7] or gastrointestinal tract[8], etc. To extend the use of microrobots inside the human body, microrobotic navigation through *densely crowded environments* remains a grand challenge.[9] Furthermore, delivering *cells in dense environments* is even more challenging as the cell viability of the transplanted cells is extremely low, and the route of cell administration is also a serious concern.[10]

Cell therapy employs live cells to treat diseases that are incurable by other treatments.[11] Recently, stem cell research has attracted much interest because these cells can differentiate into multiple progenies that could repair or replace damaged tissues.[12] Like any other therapeutic, stem cell delivery to a specific site is of prime importance. Traditionally, cells are injected directly at the target sites, which suffer many shortcomings, such as attack from the immune system, low retention, and a meager survival rate.[13] As an alternative, microrobots offer unique opportunities for cell delivery[14] as they can penetrate the inaccessible regions of the human body and deliver cargo at precise locations.[15-17] Among various types of

microrobots[18], magnetically actuated microrobots[19] are more attractive for biomedical applications as they can navigate deep into living bodies[20] under harmless weak magnetic fields.[21]

In a typical setting, magnetic microrobots of different features are loaded with the cells and transported to the target locations by guiding them under the influence of magnetic forces.[22-24] The focus of early research on microrobotic cell delivery has been the design of microrobots for cellular cargo manipulation[25, 26] and magnetic setup for microrobotic actuation.[27] Most of these experiments were performed in very dilute environments.[28] However, real biological environments are very complex and dense. Furthermore, the classical magnetic setup for driving the microrobots consists of Helmholtz coils[29] which is very useful for 2D manipulation. However, the complexity of biological systems demands microrobots to perform equally well in dense environments as well as in 2.5D[30] (navigation on top of a 2D cell layer) and 3D orientations. Both of the above-mentioned attributes can be achieved by developing more powerful actuation systems without compromising their cytocompatibility.

Magnetic tweezers manipulate magnetic particles by creating a magnetic field gradient.[31] Unlike the electromagnetic coil systems that require the microrobots to have nonreciprocal motion, magnetic tweezers can apply stronger force to the magnetic particles.[32] Magnetic tweezers also offer better motion control and enough working space.[33] Owing to these features, magnetic tweezers are very attractive candidates for microrobotic manipulation in biological environments.

In the current work, we report the transport of cells in a very dense environment populated by cells. We employ magnetic tweezers to generate the powerful force on the nickel-coated Janus microrobots, enabling them to carry cells easily in a crowded space. We first designed and fabricated the magnetic tweezer setup and then employed it for the cellular cargo manipulation. The novelty in this work is a new approach for transporting cells in a highly populated and dense environment using magnetic tweezers and nickel-coated Janus microrobots.

Experimental Section

Design and fabrication of tweezer setup

Magnetic tweezers employ electromagnetic coils and tip-shaped poles to create a magnetic field gradient, thereby exerting a magnetic force on magnetic particles when an input current is applied to the coils. [34] Single-pole magnetic tweezers are straightforward to implement, but they only generate attractive forces toward the pole tip. To enhance the degrees of freedom in applying magnetic force, we developed tri-pole magnetic tweezers. The magnetic tweezer

system we designed for the control of magnetic microrobots is illustrated in Figure 1. Its main components are divided into three sections: the yoke, poles, and coils. Initially, the yoke was designed in SolidWorks and then 3D printed using AMOLEN Metal PLA, which contains 20% Metal Iron powder. This yoke has an outer diameter of 114 mm and a thickness of 34 mm. The Metal PLA offers several benefits: it completes the magnetic circuit, enhancing the efficiency of magnetic field generation;1 it introduces high magnetic permeability to amplify the magnetic field; and it reduces the current required, thus decreasing the heat generated by the coils. Three magnetic poles, constructed from a Nickel-Iron soft ferromagnetic alloy (Mu-Metal, provided by Magnetic Shield Corporation), are inserted into the yoke. Each pole's sharp tip points toward the center, with each pole placed on the same level and at an angle of 120 degrees. The distance between two tips is 2 mm, and these poles were fabricated via laser cutting. An electromagnetic coil consisting of 600 turns of 28 AWG Enameled Copper Wire is fixed at the end of each magnetic pole.

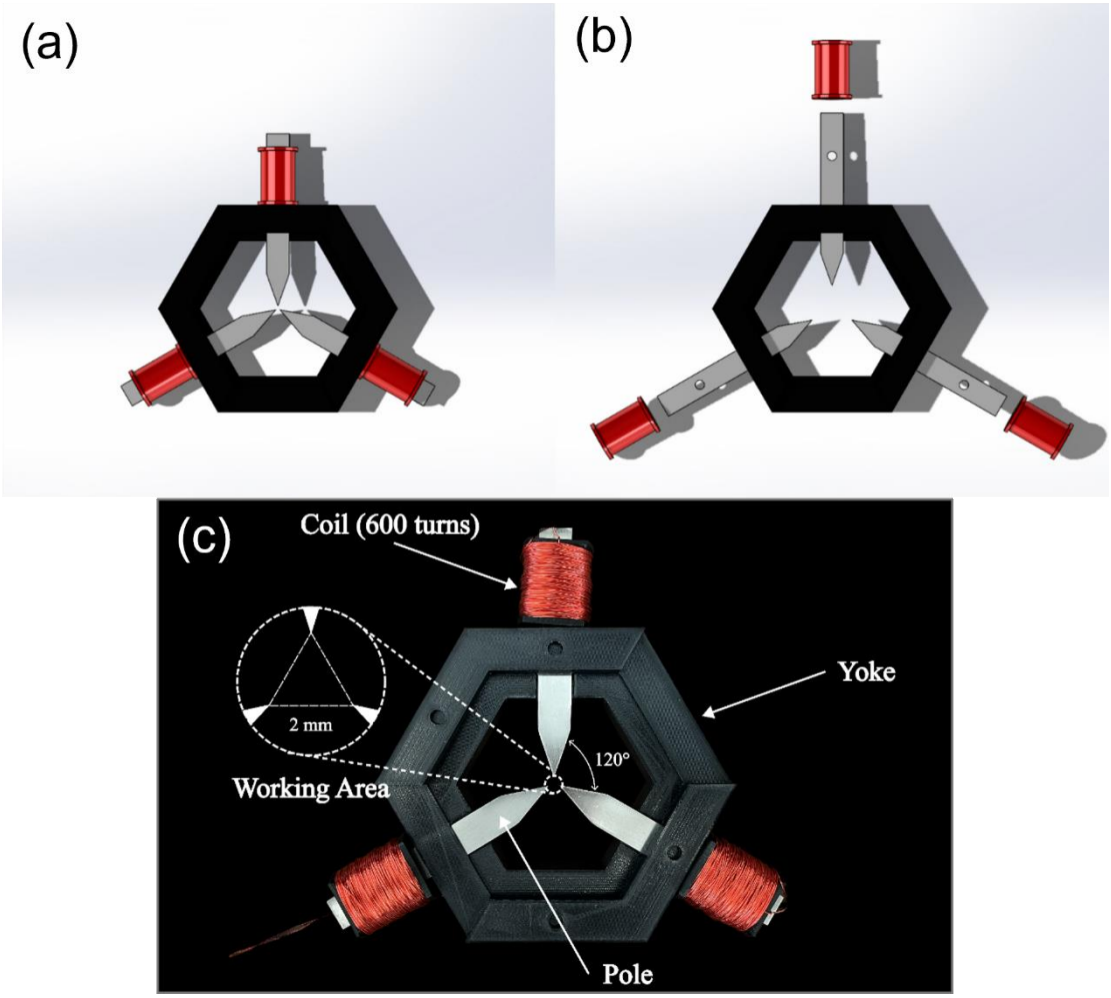

Figure 1 Experiment setup: SolidWorks model (a and b) and digital photograph (c) of the magnetic tweezers.

For precise control of the microrobots, a model was developed for the system. Figure 2 illustrates the Cartesian coordinates of this system. According to the principle of vector superposition, the magnetic force generated by any two poles can produce a combined magnetic force between them of any direction and magnitude. To achieve this, it is only necessary to regulate the magnitude of the magnetic force on each pole, which is influenced by the magnitude of the current applied. The entire Cartesian coordinate system is divided into three areas, each with two poles contributing to the superposition simultaneously.

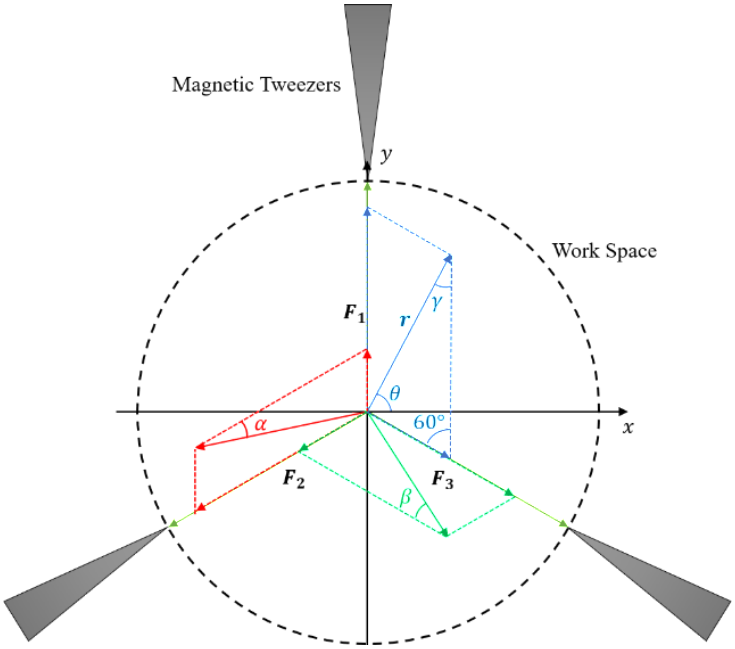

Figure 2. Schematic explanation of the working principal of magnetic tweezers.

Considering the blue lines as an example, the smaller angle of the parallelogram is 60°. The other two angles of the triangle which is the half of the parallelogram are α and β respectively.

According to the Law of Sines:[35]

$$\frac{r}{\sin\left(\frac{\pi}{3}\right)} = \frac{\|\boldsymbol{F_1}\|}{\sin(\alpha)} = \frac{\|\boldsymbol{F_2}\|}{\sin(\beta)} = \frac{\|\boldsymbol{F_3}\|}{\sin(\gamma)} \tag{1}$$

where $\boldsymbol{r}$ is the joint magnetic force vector, $r = \|\boldsymbol{r}\| = \sqrt{x^2 + y^2}$, x and y are the cartesian coordinates of $\boldsymbol{r}$, $\boldsymbol{F_1}$, $\boldsymbol{F_2}$, and $\boldsymbol{F_3}$ are the three magnetic force vector components respectively, α, β and γ which are the angles corresponding to $\boldsymbol{F_1}$, $\boldsymbol{F_2}$, and $\boldsymbol{F_3}$ respectively, they are given by:

$$\alpha = \theta + \frac{\pi}{6}, \beta = 0, \gamma = -\theta + \frac{\pi}{2}, -\frac{\pi}{6} < \theta < \frac{\pi}{2} \quad (2)$$

$$\alpha = -\theta + \frac{7\pi}{6}, \beta = \theta - \frac{\pi}{2}, \gamma = 0, \frac{\pi}{2} < \theta \leq \pi \quad (3)$$

$$\alpha = -\theta - \frac{5\pi}{6}, \beta = \theta + \frac{3\pi}{2}, \gamma = 0, -\pi < \theta < -\frac{5\pi}{6} \quad (4)$$

$$\alpha = 0, \beta = -\theta - \frac{\pi}{6}, \gamma = \theta + \frac{5\pi}{6}, -\frac{5\pi}{6} < \theta < -\frac{\pi}{6} \quad (5)$$

Hence, once we establish the coordinates of the combined magnetic force vector, we can understand its components, which have a positive correlation with the applied current. This allows us to accurately determine the amount of current we need to apply to the poles to generate the desired joint magnetic force with a specific direction and magnitude.

Fabrication of microrobots. The magnetically actuated microrobots were made of commercially obtained silica microspheres (Spherotech, Magnetic beads 4.7 μm in diameter). The particle suspension was placed on a glass slide to make a monolayer by letting it evaporate. Then these particles were made Janus by coating their one side with a 20 nm nickel layer using e-beam deposition (PVD Products). The Janus particles were recovered by mopping the glass substrate with a water-soaked lens cleaning paper. The paper was placed in a 1.5 ml vial containing 0.5 ml DI water and vortexed at high speed for a few seconds. This gave us a dilute suspension of the Janus particles. The colloids were used in experiments without any further treatment.

Assessment of Cytocompatibility. Human Embryonic Kidney cells (HEK-293 cells) were cultured in Dulbecco's Modified Essential Medium (DMEM, Gibco, Bench Stable, USA) media with 5% CO_2 and maintained at 37 °C in an incubator. All experiments were performed after third passage. Cells were seeded ($2x10^4$ cells/well) in a clear flat bottom 24-well plate (Costar, Corning, USA) and incubated in 1:1 mixture of DMEM media with 5% CO_2 at 37 °C for 24 hrs. Then, cells were treated with microrobots (4.7 μM size, 1 mg/mL) and incubated for 24 hrs. Cells were then washed and trypsinzed for Flow cytometry analysis. Propidium Iodide (PI) staining was used to assess cell death before analysis.

Results and discussion

Magnetic microrobots were manufactured by metal deposition onto a self-assembled monolayer of silica colloids.[36] Specifically, a glass slide was used as a substrate to disperse an aqueous suspension of the silica particle onto it. The suspension was evaporated without heating and a monolayer of the particles was obtained. Then a metallic layer of Ni (20 nm) was

deposited onto these particles using a dual e-beam deposition instrument. The Ni layer served as magnetic responsive material for the magnetically powered propulsion. The metal-coated particles were recovered from the glass substrate and stored in DI water at room temperature for future use. The particles were characterized by scanning electron microscopy and their representative images are shown in Figure 3. It is important to notice that a Ni layer can not be observed when SEM images are captured in normal mode as seen in Figure 3a. To observe a metal cap, we need to tilt the SEM stage and then the Janus nature of particles can be captured as shown in Figure 3b.

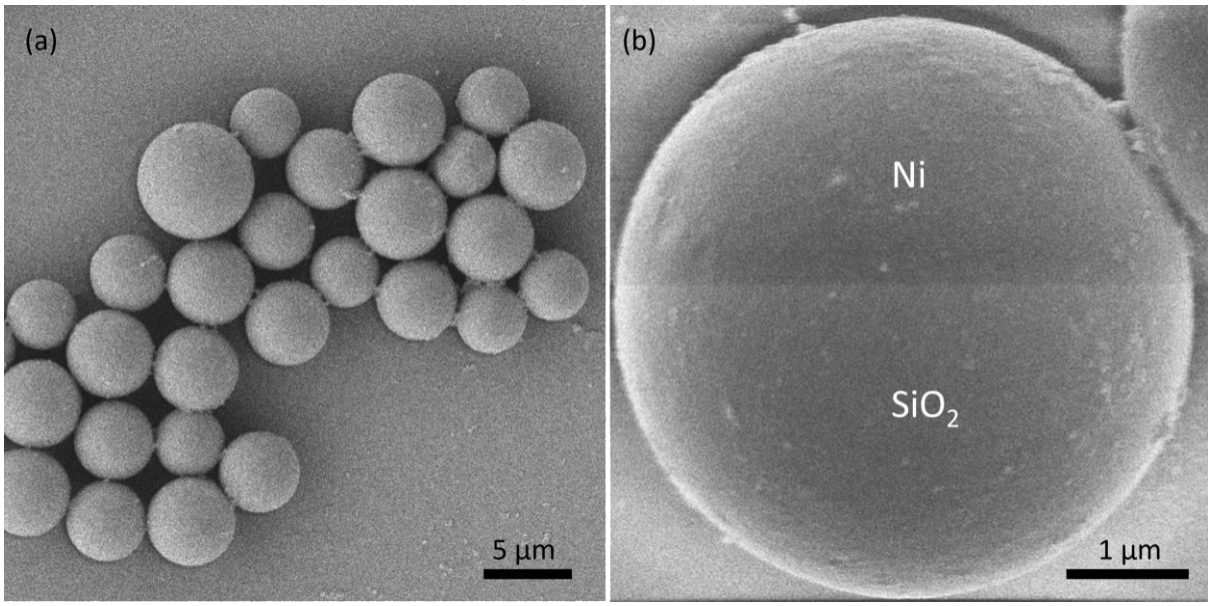

Figure 3. Morphology of the microrobots used in this study (a) wider field of view SEM image and (b) high magnification SEM image taken with tilted stage.

To study the motion of these magnetically responsive Janus microrobots, dilute particle suspensions were dropped onto a plasma-cleaned glass slide.[37] The particles showed a Brownian motion in the absence of a magnetic field. When the magnetic field was applied to these particles, they all responded to it and moved in the specified direction. The direction of motion was controlled by changing the direction of the applied magnetic field. To move the microrobots in a specific direction, we applied the current to the coils attached to specific poles. For example, in Figure 4 and movie S1, the particles were moved toward right at 0 to 2 sec by activating the coils attached to the right pole. For better visualization, one microrobot is encircled to track its position. All other microrobots follow the same motion direction as the applied field is global in nature.

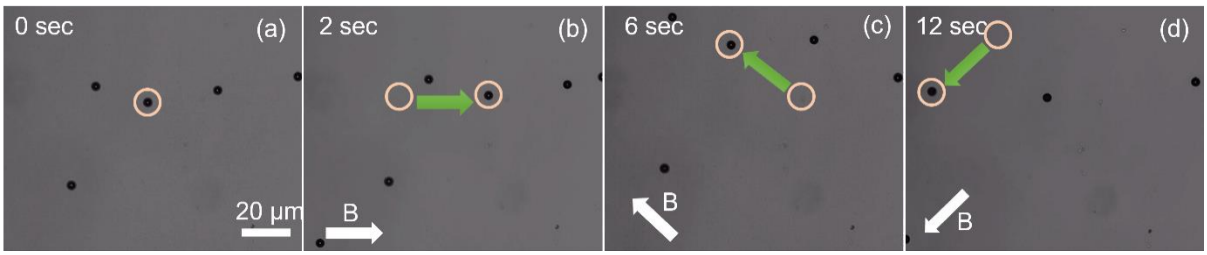

Figure 4. Motion of microbots controlled by magnetic tweezers. One microrobot is encircled to better visualize the motion of all microrobots controlled by changing the direction of the applied magnetic field. Change in microrobot's position is shown by a green arrow. (a) There is no motion at 0 sec, (b) the microrobots move from left to write at 2 sec, (c) the microrobots are moved towards the upper left corner at 6 sec, and (d) the microrobots are moved towards lower left corner at 12 sec.

Biocompatibility is one of the important factors while designing microrobots.[38] In addition to being non-toxic, microrobots should not release any chemicals or by-products that are going to affect results during experiments.[10] To assess the cytocompatibility of our microrobots, HEK-293 cells were incubated with microrobots for 24 hrs. Flow cytometry data suggested microrobots-treated cells were nontoxic when compared with the control cells without microrobots. The percentage of dead cells in the flow cytometry data was l.5 % demonstrating that the microrobots were cytocompatible (Figure 5). This data confirmed that our magnetic microrobots are suitable for further modification and biological experiments.

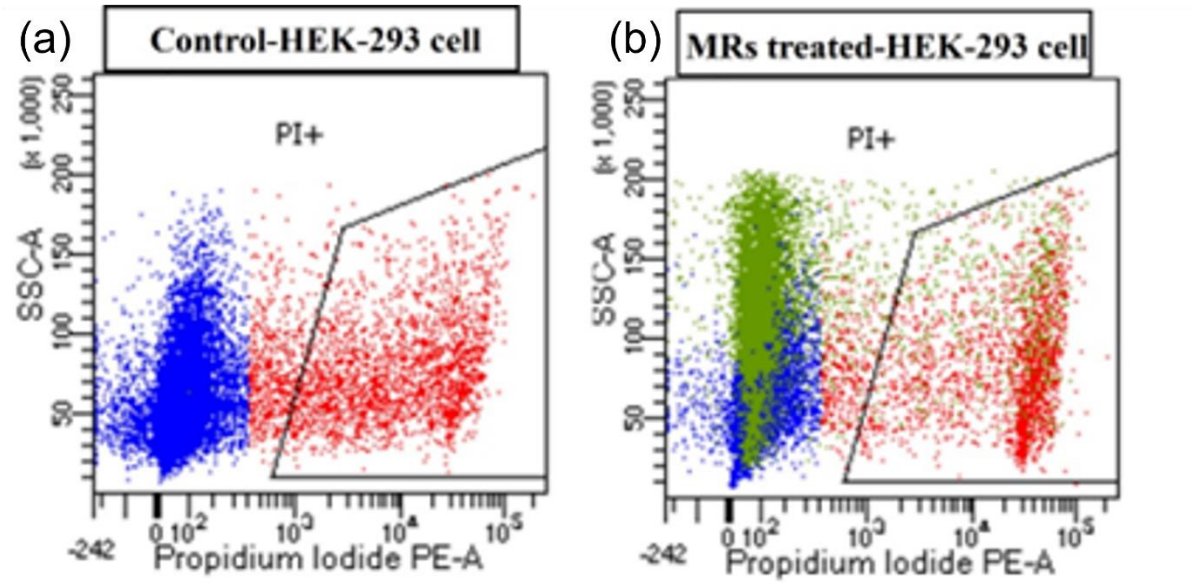

Samples	Percentage cell death (%)
Control	8.2
MRs-treated	9.7

Figure 5. Cytocompatibility of Microrobots in HEK-293 cells Flow cytometry data showed that after 24 hrs, the cell death increased from 8.2% in control experiment (a) to 9.7% cell death in the case of CF-labeled Microrobots with HEK-293 cells (b).

Next, we investigated the magnetic tweezer-controlled microrobots for transporting cells in a dense environment. A concentrated suspension of HEK-293 cells was mixed with a dilute suspension of microrobots. The mixture was homogenized by a gentle pipette-mixing. The mixture was dropped onto a plasma-cleaned glass slide. Next, we located the microrobots attached to the cells to test them for transportation. As an example, as shown in Figure 6 and video S2, a cell doublet was found attached to the microrobots. A cell doublet is an interesting cargo example as it can show both translational as well rotational motion. We demonstrated this by first moving the cell doublet toward the upper left corner (at 0-5 sec). After moving the doublet for one body length, we rotated it by 45 degree (at 10 sec), and then moved it toward the upper right corner by two body lengths (at 15 sec). These results show the magnetically controlled transportation of cells through a densely populated environment.

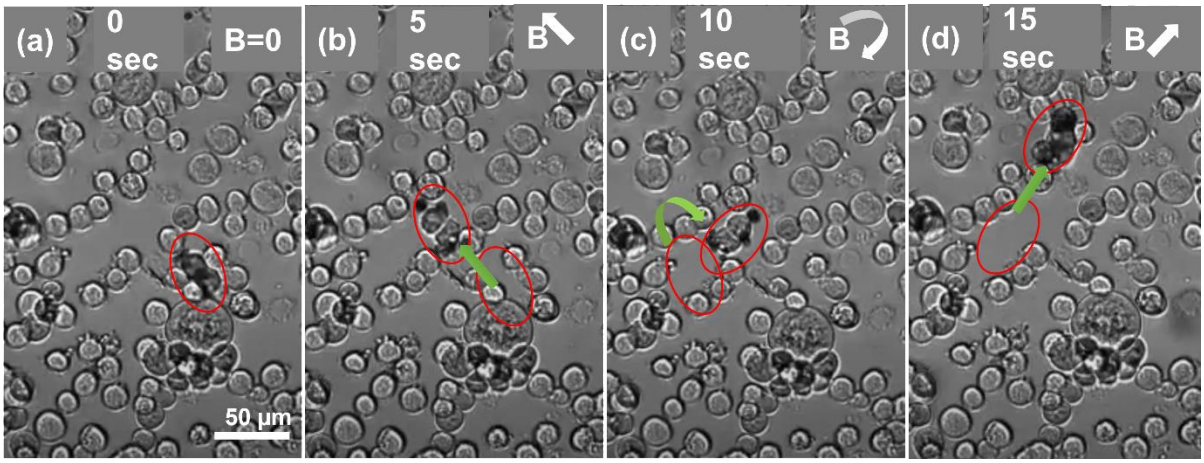

Figure 6. Microrobots carrying a cell doublet via the magnetic field. The cell doublet is transported one body length (0-5 sec, (a) and (b)), rotated 45 degree (10 sec, (c)), then transported two body lengths (15 sec, (d)). Green arrows show the change in position of the cell doublet. Red ellipsoids indicate the cell location before and after the transportation step, respectively.

Conclusion

In summary, we present the development of a microrobotic system designed to transport cells in a densely crowded cellular environment. The system comprises of magnetically powered tweezers and Ni-coated Janus microspheres. To construct the system, we designed, and 3D printed the magnetic tweezer setup, which was mounted on an inverted microscope. The microrobots were fabricated by depositing Ni on commercially available silica microspheres. Human Embryonic Kidney cells were used as a model cargo and to create the dense environment. Our experiments successfully demonstrated the transportation of cells through the crowded environment using magnetically actuated microrobots. This work provides a proof-of-concept for the practical application of magnetic microrobots in a biological setting. We anticipate that this research will contribute to the development of improved biomedical therapeutics utilizing microrobots.

References

[1] Sitti, M., Ceylan, H., Hu, W., Giltinan, J., Turan, M., Yim, S. and Diller, E. Biomedical Applications of Untethered Mobile Milli/Microrobots. *Proceedings of the IEEE*, 103, 2 2015), 205-224.

[2] Erkoc, P., Yasa, I. C., Ceylan, H., Yasa, O., Alapan, Y. and Sitti, M. Mobile Microrobots for Active Therapeutic Delivery. *Advanced Therapeutics*, 2, 1 2019), 1800064.

[3] Song, X., Sun, R., Wang, R., Zhou, K., Xie, R., Lin, J., Georgiev, D., Paraschiv, A.-A., Zhao, R. and Stevens, M. M. Puffball-Inspired Microrobotic Systems with Robust Payload,

Strong Protection, and Targeted Locomotion for On-Demand Drug Delivery. *Advanced Materials*, 34, 43 2022), 2204791.
[4] Cui, J., Huang, T.-Y., Luo, Z., Testa, P., Gu, H., Chen, X.-Z., Nelson, B. J. and Heyderman, L. J. Nanomagnetic encoding of shape-morphing micromachines. *Nature*, 575, 7781 (2019/11/01 2019), 164-168.
[5] Tottori, S., Zhang, L., Qiu, F., Krawczyk, K. K., Franco-Obregón, A. and Nelson, B. J. Magnetic Helical Micromachines: Fabrication, Controlled Swimming, and Cargo Transport. *Advanced Materials*, 24, 6 2012), 811-816.
[6] Yan, X., Zhou, Q., Vincent, M., Deng, Y., Yu, J., Xu, J., Xu, T., Tang, T., Bian, L., Wang, Y.-X. J., Kostarelos, K. and Zhang, L. Multifunctional biohybrid magnetite microrobots for imaging-guided therapy. *Sci. Robot.*, 2, 12 2017), 1155.
[7] Wu, Z., Troll, J., Jeong, H.-H., Wei, Q., Stang, M., Ziemssen, F., Wang, Z., Dong, M., Schnichels, S., Qiu, T. and Fischer, P. A swarm of slippery micropropellers penetrates the vitreous body of the eye. *Science Advances*, 4, 11 2018), eaat4388.
[8] Wu, Z., Li, L., Yang, Y., Hu, P., Li, Y., Yang, S.-Y., Wang, L. V. and Gao, W. A microrobotic system guided by photoacoustic computed tomography for targeted navigation in intestines in vivo. *Science Robotics*, 4, 32 2019), eaax0613.
[9] Ceylan, H., Yasa, I. C., Kilic, U., Hu, W. and Sitti, M. Translational prospects of untethered medical microrobots. *Progress in Biomedical Engineering*, 1, 1 (2019/07/16 2019), 012002.
[10] Choi, J., Hwang, J., Kim, J.-y. and Choi, H. Recent Progress in Magnetically Actuated Microrobots for Targeted Delivery of Therapeutic Agents. *Advanced Healthcare Materials*, 10, 6 2021), 2001596.
[11] Gage, F. H. Cell therapy. *Nature*, 392(1998/04// 1998), 18-24.
[12] Daley, G. Q. The Promise and Perils of Stem Cell Therapeutics. *Cell Stem Cell*, 10, 6 (2012/06/14/ 2012), 740-749.
[13] Golpanian, S., Schulman, I. H., Ebert, R. F., Heldman, A. W., DiFede, D. L., Yang, P. C., Wu, J. C., Bolli, R., Perin, E. C., Moyé, L., Simari, R. D., Wolf, A. and Hare, J. M. Concise Review: Review and Perspective of Cell Dosage and Routes of Administration From Preclinical and Clinical Studies of Stem Cell Therapy for Heart Disease. *STEM CELLS Translational Medicine*, 5, 2 2016), 186-191.
[14] Jeon, S., Kim, S., Ha, S., Lee, S., Kim, E., Kim, S. Y., Park, S. H., Jeon, J. H., Kim, S. W., Moon, C., Nelson, B. J., Kim, J.-y., Yu, S.-W. and Choi, H. Magnetically actuated microrobots as a platform for stem cell transplantation. *Science Robotics*, 4, 30 2019), eaav4317.
[15] Nelson, B. J., Kaliakatsos, I. K. and Abbott, J. J. Microrobots for Minimally Invasive Medicine. *Annual Review of Biomedical Engineering*, 12, 1 2010), 55-85.
[16] Lee, H., Kim, D.-i., Kwon, S.-h. and Park, S. Magnetically Actuated Drug Delivery Helical Microrobot with Magnetic Nanoparticle Retrieval Ability. *ACS Applied Materials & Interfaces*, 13, 17 (2021/05/05 2021), 19633-19647.
[17] Martel, S. Magnetic therapeutic delivery using navigable agents. *Therapeutic Delivery*, 5, 2 2014), 189-204.
[18] Ceylan, H., Giltinan, J., Kozielski, K. and Sitti, M. Mobile microrobots for bioengineering applications. *Lab on a Chip*, 17, 10 2017), 1705-1724.
[19] Akolpoglu, M. B., Alapan, Y., Dogan, N. O., Baltaci, S. F., Yasa, O., Aybar Tural, G. and Sitti, M. Magnetically steerable bacterial microrobots moving in 3D biological matrices for stimuli-responsive cargo delivery. *Science Advances*, 8, 28 2022), eabo6163.
[20] Simaan, N., Yasin, R. M. and Wang, L. Medical Technologies and Challenges of Robot-Assisted Minimally Invasive Intervention and Diagnostics. *Annual Review of Control, Robotics, and Autonomous Systems*, 1, 1 2018), 465-490.
[21] Shah, Z. H., Wu, B. and Das, S. Multistimuli-responsive microrobots: A comprehensive review. *Front Robot AI*, 9(2022-November-07 2022), 1027415.

[22] Wei, T., Liu, J., Li, D., Chen, S., Zhang, Y., Li, J., Fan, L., Guan, Z., Lo, C.-M., Wang, L., Man, K. and Sun, D. Development of Magnet-Driven and Image-Guided Degradable Microrobots for the Precise Delivery of Engineered Stem Cells for Cancer Therapy. *Small*, 16, 41 2020), 1906908.
[23] Jeon, S., Park, S. H., Kim, E., Kim, J.-y., Kim, S. W. and Choi, H. A Magnetically Powered Stem Cell-Based Microrobot for Minimally Invasive Stem Cell Delivery via the Intranasal Pathway in a Mouse Brain. *Advanced Healthcare Materials*, 10, 19 2021), 2100801.
[24] Kim, S., Qiu, F., Kim, S., Ghanbari, A., Moon, C., Zhang, L., Nelson, B. J. and Choi, H. Fabrication and Characterization of Magnetic Microrobots for Three-Dimensional Cell Culture and Targeted Transportation. *Advanced Materials*, 25, 41 2013), 5863-5868.
[25] Sanchez, S., Solovev, A. A., Schulze, S. and Schmidt, O. G. Controlled manipulation of multiple cells using catalytic microbots. *Chemical Communications*, 47, 2 2011), 698-700.
[26] Balasubramanian, S., Kagan, D., Jack Hu, C.-M., Campuzano, S., Lobo-Castañon, M. J., Lim, N., Kang, D. Y., Zimmerman, M., Zhang, L. and Wang, J. Micromachine-Enabled Capture and Isolation of Cancer Cells in Complex Media. *Angew Chem Intl Ed*, 50, 18 2011), 4161-4164.
[27] Zhou, H., Mayorga-Martinez, C. C., Pané, S., Zhang, L. and Pumera, M. Magnetically Driven Micro and Nanorobots. *Chemical Reviews*, 121, 8 (2021/04/28 2021), 4999-5041.
[28] Steager, E. B., Selman Sakar, M., Magee, C., Kennedy, M., Cowley, A. and Kumar, V. Automated biomanipulation of single cells using magnetic microrobots. *The International Journal of Robotics Research*, 32, 3 2013), 346-359.
[29] Yang, Z. and Zhang, L. Magnetic Actuation Systems for Miniature Robots: A Review. *Advanced Intelligent Systems*, 2, 9 2020), 2000082.
[30] Ago, H., Okada, S., Miyata, Y., Matsuda, K., Koshino, M., Ueno, K. and Nagashio, K. Science of 2.5 dimensional materials: paradigm shift of materials science toward future social innovation. *Science and Technology of Advanced Materials*, 23, 1 (2022/12/31 2022), 275-299.
[31] Gosse, C. and Croquette, V. Magnetic Tweezers: Micromanipulation and Force Measurement at the Molecular Level. *Biophysical Journal*, 82, 6 (2002/06/01/ 2002), 3314-3329.
[32] Zhang, X., Kim, H., Rogowski, L. W., Sheckman, S. and Kim, M. J. *Novel 3D magnetic tweezer system for microswimmer manipulations*. City, 2017.
[33] de Vries, A. H. B., Krenn, B. E., van Driel, R. and Kanger, J. S. Micro Magnetic Tweezers for Nanomanipulation Inside Live Cells. *Biophysical Journal*, 88, 3 (2005/03/01/ 2005), 2137-2144.
[34] Zhang, Z., Huang, K. and Menq, C. H. Design, Implementation, and Force Modeling of Quadrupole Magnetic Tweezers. *IEEE/ASME Transactions on Mechatronics*, 15, 5 2010), 704-713.
[35] Coxeter, H. S. M. and Greitzer, S. L. *Geometry revisited*. Maa, 1967.
[36] Wang, H. and Pumera, M. Fabrication of Micro/Nanoscale Motors. *Chemical Reviews*, 115, 16 (2015/08/26 2015), 8704-8735.
[37] Chen, X., Zhou, C. and Wang, W. Colloidal Motors 101: A Beginner's Guide to Colloidal Motor Research. *Chem. Asian J.*, 14, 14 (Jul 15 2019), 2388-2405.
[38] Chen, W., Zhou, H., Zhang, B., Cao, Q., Wang, B. and Ma, X. Recent Progress of Micro/Nanorobots for Cell Delivery and Manipulation. *Advanced Functional Materials*, 32, 18 2022), 2110625.